Digital Pre-Distortion for Mach–Zehnder Modulators in IMDD Optical Systems

Meng Yang, Aiying Yang*, Peng Guo, Zhe Zhao, Tianjia Xu, Wenkai Wan
Key Laboratory of Photonics Information Technology, Ministry of Industry and Information Technology, School of Optics and Photonics, Beijing Institute of Technology, Beijing 100081, China
*yangaiying@bit.edu.cn

***Abstract*—We present a digital pre-distortion (DPD) scheme to compensate for Mach-Zehnder modulator (MZM) in intensity modulation and direct detection (IMDD) optical systems. In our DPD scheme, the modulator driving signal is pre-distorted to mitigate the distortion introduced by the nonlinear transfer function of the MZM. The DPD scheme is performed in two steps: first, the coefficient of the nonlinear impairment is computed using the predefined mathematical models of the optical back-to-back (BTB) IMDD system; second, an adjusting factor of the DPD is introduced and optimized to obtain the best performance of the system. Both numerical simulations and experimental demonstrations were conducted to assess the DPD gain for feed-forward equalization (FFE) and third-order Volterra filter equalization (VFE), respectively. In experimental C-band 20 GBaud four-level pulse amplitude modulation (PAM4) IMDD optical BTB system. DPD scheme can obtain 2.4 dB and 1.2 dB improvement of receiver sensitivity for FFE and VFE at a bit error ratio (BER) for 1×10^{-3}, respectively.**

***Index Terms*—IMDD optical system, digital pre-distortion, Mach-Zehnder modulator**

I. Introduction

In recent years, short-reach optical transmission systems become the fastest growing section of the optical communication market [1]–[4]. Intensity modulation and direct detection (IMDD) has been adopted to short-reach optical systems due to its advantage of small form factors, low cost and low power consumption [5]. Besides, four-level pulse amplitude modulation (PAM4) is a promising format for IMDD systems, which has also been elected as a standard format for 400-G Ethernet [6]–[8].

For short-reach IMDD optical systems, the modulation nonlinearity of Mach-Zehnder modulator (MZM) will damage the signal quality, especially in high order modulation formats and high baud rates systems. This distortion could interplay with chromatic dispersion (CD) after the square-law detection of the photodetector (PD), further deteriorating signal quality [9]. Digital pre-distortion (DPD) at the transmitter has been investigated to compensate for nonlinear distortion in optical transmission systems [10]–[12]. H. Jiang, et al. proposed a practical arcsin iterative algorithm to compensate for in-phase and quadrature (IQ) MZM with finite extinction ratio (ER) [10]. G. Li, et al. used nonlinear equalizer to pre-equalize the linear and nonlinear impairments in O-baud 25 GBaud PAM4 IMDD optical system [11]. H. Jiang, et al. used Volterra filter equalizer (VFE) in the transmitter side to mitigate transmitter-side nonlinear distortion in optical transmissions [12].

This work was supported by the National Natural Science Foundation of China under Grant 61427813, the Open Fund of IPOC (BUPT) under Grant IPOC2018B003.

In this paper, we propose a digital pre-distortion scheme to compensate for the third-order nonlinear impairment introduced by MZM in IMDD optical system. The DPD scheme is performed in two steps: first, the coefficient of the third-order nonlinear impairment is computed using the predefined mathematical models of the optical back-to-back (BTB) IMDD system; second, an adjusting factor of the DPD is introduced and optimized to obtain the best performance of the system. The DPD gain was assessed in the simulation C-band 25 GBaud PAM4 IMDD optical system over 20 km standard single-mode fiber (SSMF) transmission and experimental C-band 20 GBaud PAM4 IMDD optical BTB system, respectively.

II. Digital pre-distortion for MZM

In the IMDD optical system, the output optical field signals of the MZM can be expressed as

$$E_{\mathrm{out}}(t)=\cos(\pi\frac{s(t)+s_{\mathrm{dc}}}{2v_\pi})E_{\mathrm{in}}(t) \tag{1}$$

where $E_{\mathrm{in}}(t)$ is the input optical field of the MZM, v_π is the half-wave of the MZM, $s(t)$ is the driving signal of MZM, s_{dc} is the DC bias. When the DC bias is at the quadrature point of the MZM s_{dc} = $v_\pi/2$, the output optical field of the MZM can be written as

$$E_{\mathrm{out}}(t)=\cos(\frac{\pi}{2v_\pi}s(t)+\frac{\pi}{4})E_{\mathrm{in}}(t) \tag{2}$$

In optical BTB system, the current intensity of the PD can be described as

$$i(t)=\left|E_{\mathrm{out}}(t)\right|^2=\cos^2(\frac{\pi}{2v_\pi}s(t)+\frac{\pi}{4})\left|E_{\mathrm{in}}(t)\right|^2 \tag{3}$$

The Taylor expression of (3) is

$$i(t)=\frac{1}{2}(1-\frac{\pi}{v_\pi}s(t)+\frac{1}{3!}\frac{\pi^3}{v_\pi^3}s^3-\frac{1}{5!}\frac{\pi^5}{v_\pi^5}s_+^5.....)\left|E_{\mathrm{in}}(t)\right|^2 \tag{4}$$

Equation (4) predicts that the signal will distorted by the nonlinear transfer function of the MZM in IMDD optical system. In our DPD scheme, only considering the third-order

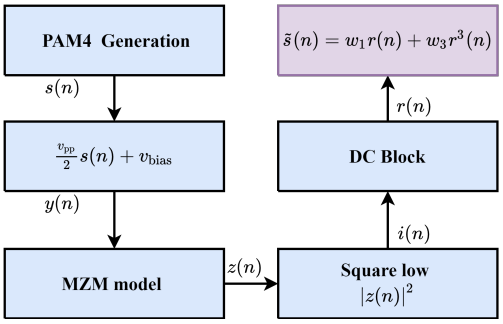

Fig. 1: The calculation and training of coefficients w_1 and w_3 using LMS algorithms.

nonlinear impairment, the digital pre-distorted driving signal of the MZM is expressed as

$$s_{\mathrm{DPD}}(n) = w_1 s(n) + w_3 s^3(n) \tag{5}$$

Introducing an adjusting factor μ of the DPD, the real digital pre-distorted driving signal is expressed as

$$y(n) = s(n) + \mu(s_{\mathrm{DPD}}(n) - s(n)) \tag{6}$$

The coefficient w_1 and w_3 are computed using the predefined models of the optical BTB IMDD system as shown in Fig. 1. v_{pp} is the peak-to-peak amplitude of the driving signal. v_{bias} is amplitude of the DC bias. Using least mean square (LMS) algorithm, the coefficients w_1 and w_3 are obtained by minimizing the mean square error (MSE) between the desired PAM4 symbols $s(n)$ and the obtained PAM4 symbols $\tilde{s}(n)$.

III. Simulation Setup and Results Analysis

A. Simulation setup

Fig. 2 shows the simulation setup for C-band 25 GBaud PAM4 IMDD optical system. The simulation system was built using commercial software VPItransmissionMakerTM 9.5. At the transmitter-side, the generated electrical PAM4 symbol was adjusted by a RF amplifier. The number of the PAM4 symbols was 131072. The VPI model "LaserDriver" emulates the amplitude of the driving signal and DC bias. The output signal of the "LaserDriver" is equal to $y(n) * \mathbf{DriveAmplitude} + \mathbf{Bias}$. A laser with central wavelength of 1550 nm was employed to generate optical carrier. A MZM was used to modulate the electrical signal into optical domain. The launch power into fiber was 6 dBm. To ensure accuracy in the simulation of the fiber forward propagation, the overall signal field was sampled at 8 samples per symbol. At the receiver-side, a variable optical attenuator (VOA) was applied to adjust receiver optical power and an avalanche photodetector (APD) was employed to achieve photoelectric conversion. After photoelectric conversion, the signal was captured for offline digital signal processing (DSP). Table. I lists the parameter of the simulation system.

Both transmitter-side and receiver-side DSPs were performed offline. At the transmitter-side DSP, if DPD is used,

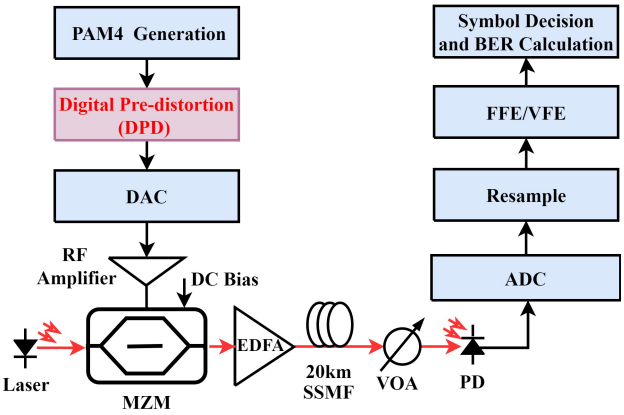

Fig. 2: The simulation setup for the C-band 25 GBaud PAM4 IMDD 20 km SSMF optical transmission system. DAC: digital-to-analog converter, MZM: Mach-Zehnder modulator, SSMF: standard single-mode fiber, PD: photodetector, VOA: variable optical attenuator, ADC: analog-to-digital converter.

TABLE I: The parameters of the simulation system

Parameters	Value
Laser Average Power	0 dBm
Laser Wavelength	1550 nm
DriveAmplitude	0.5 V
Bias	0.5 V
EDFA Output Power	6 dBm
EDFA Noise Figure	4 dB
Fiber Length	20 km
Disperson Coefficient	16×10^{-6} s/m^2
APD Responsivity	2 A/W
APD 3 dB Bandwidth	21 GHz
APD ThermalNoise	10^{-12} A/ $\sqrt{\mathrm{Hz}}$

the PAM4 symbols were distorted using (6). At the receiver-side DSP, the received PAM4 symbols were down-sampled to 1 samples per symbol. Then feed-forward equalization (FFE) was applied to compensate for the linear impairments, or third-order VFE was used to compensate for the linear and nonlinear impairments [3]. For the purpose of performance comparison, we focus on the following DSP cases: 1) receiver side FFE; 2) receiver side third-order VFE; 3) transmitter side DPD together with receiver side FFE, namely DPD+FFE; 4) transmitter side DPD together with receiver side VFE, namely DPD+VFE.

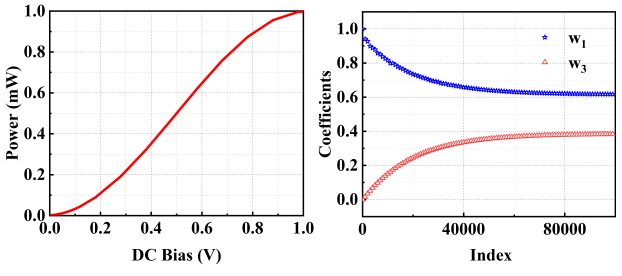

Fig. 3: (a) The simulation measured transfer function of the MZM and (b) the training results of coefficients w_1 and w_3 using LMS algorithms.

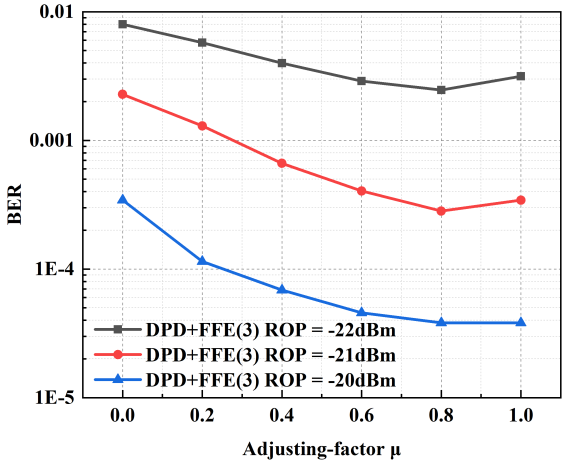

Fig. 4: The BER performance of DPD+FFE(3) versus adjusting factor μ at different receiver optical power in the simulation C-band 25 GBaud PAM4 optical BTB system.

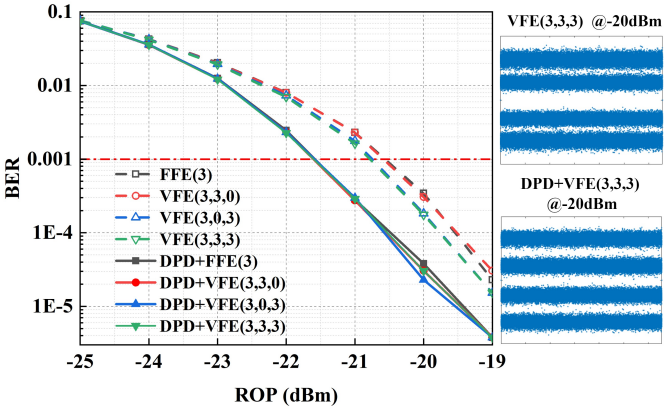

Fig. 5: The BER performance versus receiver optical power from -25 dBm to -19 dBm and the amplitude of the PAM4 symbols with VFE(3,3,3) and DPD+VFE(3,3,3) at -20 dBm in the simulation C-band 25 GBaud PAM4 optical BTB system.

B. Simulation results and analysis

Firstly, we studied the simulation measured transfer function of the MZM in Fig. 2, and the results were shown in Fig. 3(a). The output power of the MZM can be fitted as

$$P_{\mathrm{mW}} = -1.91 s_{\mathrm{dc}}^3 + 2.89 s_{\mathrm{dc}}^2 + 0.03 s_{\mathrm{dc}} \tag{7}$$

Then, the coefficient w_1 and w_3 were computed using the predefined model in Fig. 1. The optimized value of the coefficient w_1 and w_3 were 0.62 and 0.38, as shown in Fig. 3(b).

Fig. 4 shows the BER performance of DPD+FFE(3) versus adjusting factor μ from 0 to 1 at different receiver optical power (ROP) in the simulation C-band 25 GBaud PAM4 optical BTB system. $\mu = 0$ means without DPD. It depicts that the optimal BER performance was obtained at $\mu = 0.8$ and the DPD achieved better BER performance.

Fig. 5 shows the BER performance of the four cases versus ROP from -25 dBm to -19 dBm in simulation C-band 25 GBaud PAM4 optical BTB system. The adjusting factor of DPD was $\mu = 0.8$. The dotted line indicates without DPD, and solid line indicates with DPD in the transmitter-side. As Fig. 5 shows, the receiver sensitivity of FFE (3) and VFE(3,3,0) both were -20.6 dBm at a bit error ratio (BER) of 1×10^{-3}. VFE(3,0,3) increased the receiver sensitivity from -20.6 dBm to -20.8 dBm. And VFE(3,3,3) can not further improve receiver sensitivity. Therefore, in our optical BTB IMDD simulation system, third-order nonlinear impairment is the mainly impairments. With DPD in the transmitter-side, DPD+FFE(3) can increase the receiver sensitivity from -20.8 dBm to -21.6 dBm. It means that DPD can obtain 0.8 dB improvement of the receiver sensitivity. Therefore, the DPD scheme can achieve better transmission performance compared with post-equalization. Note that DPD+VFE can not further improve the BER performance, indicating that our digital pre-distortion scheme can effectively compensate for the nonlinear impairment introduced by MZM.

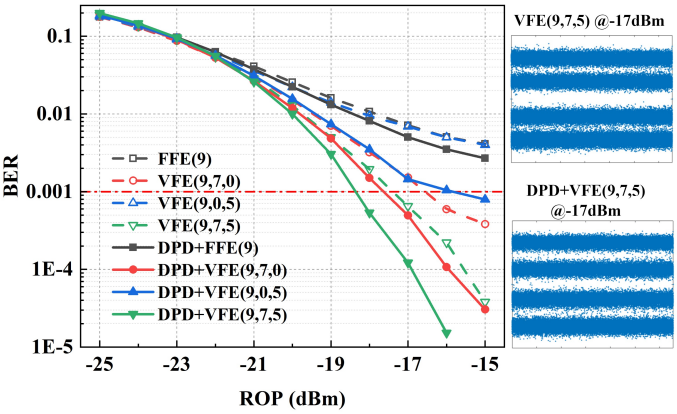

Fig. 6: The BER performance versus receiver optical power from -25 dBm to -15 dBm and the amplitude of the PAM4 symbols with VFE(9,7,5) and DPD+VFE(9,7,5) at -17 dBm in the simulation C-band 25 GBaud PAM4 optical 20 km SSMF system.

Fig. 6 shows the BER performance of the four cases versus ROP from -25 dBm to -15 dBm in simulation C-band 25 GBaud PAM4 optical system over 20 km SSFM transmission. The adjusting factor of DPD was $\mu = 0.8$. The dotted line indicates without DPD, and solid line indicates with DPD in the transmitter-side. As Fig. 6 shows, at -17 dBm receiver optical power, the BER of FFE(9) only reached 7.1×10^{-3}. VFE(9,7,0) can reduce the BER to 1.5×10^{-3}. It is because that 20 km SSMF transmission introduced second-order nonlinear impairment, namely signal-dispersion beat interference. VFE(9,7,5) can further reduce BER to 6.5×10^{-4}. The DPD+VFE(9,7,5) can reduce the BER from 6.5×10^{-4} to 6.9×10^{-5}. Compared with VFE(9,7,5), DPD+VFE(9,7,5) can improve the receiver sensitivity from -17.4 dBm to -18.4 dBm at a BER of 1×10^{-3}. It means that our DPD scheme can obtain 1 dB receiver sensitivity improvement.

IV. Experimental setup and results analysis

A. Experimental setup

The experimental setup of the C-band 20 GBaud PAM4 optical BTB system and corresponding DSP was shown in Fig. 7 (a). We use a 25 GSa/s 10-bit arbitrary waveform generator (AWG) and a RF amplitude (SHF M834B) with 15 dB gain to drive the MZM. The 3-dB bandwidth of the AWG and RF amplifier is about 10 GHz and 34 GHz, respectively. The MZM has a 6 dB insertion loss and biased at its quadrature point 3.2 V, as shown in Fig. 7 (b). The 3-dB bandwidth of MZM is 25 GHz. A 1552 nm laser source is employed with an output power of 12 dBm. After modulation, the optical launched power is about 2.6 dBm. At the receiver side, a variable optical attenuator (VOA) is employed to control the optical signal power before the photodetector. A Finisar PD with a transimpedance amplifier (TIA) is used for optical-to-electrical conversion. Finally, the received electrical signal is digitized by a 100 GSa/s Tektronix digital phosphor oscilloscope (DPO) with a 25 GHz bandwidth.

Both transmitter-side and receiver-side DSPs were performed offline. At the transmitter-side DSP, the PAM4 symbols were the same as those in simulation. If DPD is used, the PAM4 symbols were distorted using (6). The value of the coefficient w_1 and w_3 were 0.62 and 0.38, as shown in Fig. 3(b). Finally, the signal was resampled to the AWG with 20 GSa/s sampling rate. At the receiver-side DSP, the signal was first resampled to 1 samples/symbol. After synchronization, FFE was applied to compensate for linear impairments, or VFE was used to compensate for the linear and nonlinear impairments. For the purpose of performance comparison, we focus on the following DSP cases: 1) FFE; 2)VFE; 3) DPD+FFE; 4) DPD+VFE.

B. Experimental results and analysis

Fig. 8 shows the BER performance of DPD+FFE(7) versus adjusting factor μ from 0 to 1 at different ROP in experimental C-baud 20 GBaud PAM4 optical BTB system. $\mu = 0$ means without digital DPD. It depicts that the optimal BER performance is obtained at $\mu = 0.8$ and the DPD scheme achieved better BER performance.

Fig. 9 shows the BER performance of the four cases versus ROP from -14 dBm to -7 dBm in experimental C-band 20 GBaud PAM4 optical BTB system.The dotted line indicates without DPD, and solid line indicates with DPD in the transmitter-side. As Fig. 9 shows, the receiver sensitivity of FFE(7) was -9.7 dBm at a BER of 1×10^{-3}. VFE(7,3,3) can increase the receiver sensitivity from -9.7 dBm to -10.9 dBm. DPD+FFE (7) can improve the receiver sensitivity from -9.7 dBm to -12.1 dBm compared with FFE (7). It means that DPD can obtain 2.4 dB improvement of the receiver sensitivity for FFE. DPD+VFE (7,3,3) can improve the receiver sensitivity from -10.9 dBm to -12.1 dBm compared with VFE (7,3,3). It means that DPD can obtain 1.2 dB improvement of the receiver sensitivity for VFE. Therefore, our DPD scheme can effectively compensate for the nonlinear impairment introduced by MZM.

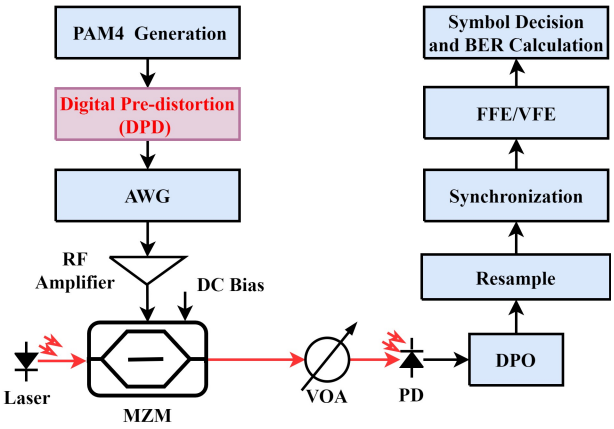

(a)

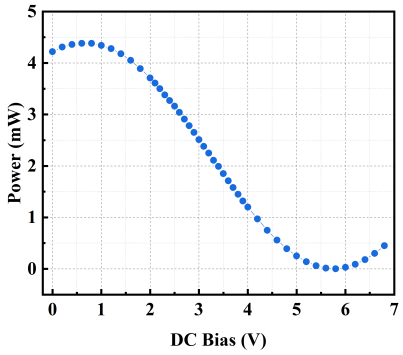

(b)

Fig. 7: (a) The experimental setup for the C-band 20 Gbaud PAM4 IMDD optical BTB system and (b) experimental measured transfer function of MZM. AWG: arbitrary waveform generator, DPO: digital phosphor oscilloscope.

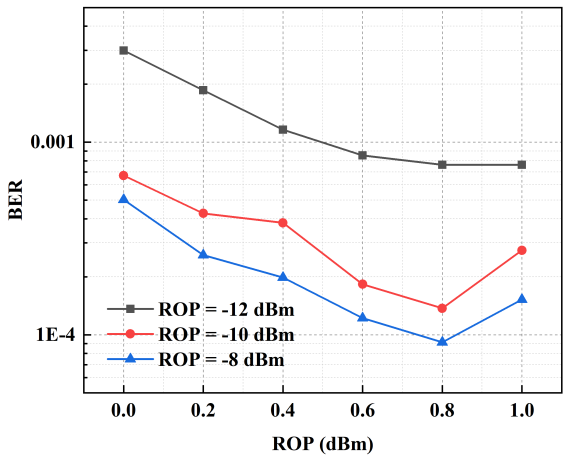

Fig. 8: The BER performance of DPD+FFE(7) versus adjusting factor μ at different receiver optical power in the experimental C-baud 20 GBaud PAM4 optical BTB system.

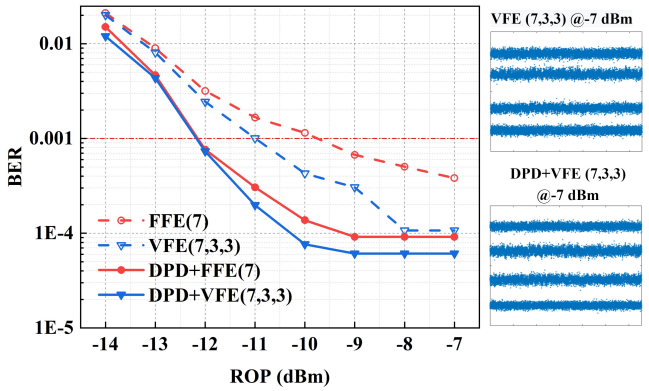

Fig. 9: The BER performance versus receiver optical power from -14 dBm to -7 dBm and the amplitude of the PAM4 symbols with VFE(7,3,3) and DPD+VFE(7,3,3) at -7 dBm in experimental C-baud 20 GBaud PAM4 optical BTB system.

CONCLUSION

We propose a digital pre-distortion scheme to compensate for the third-order nonlinear impairment introduced by MZM in IMDD optical system. The DPD gain was assessed in the simulation C-band 25 GBaud PAM4 IMDD optical system over 20 km SSMF transmission and experimental C-band 20 GBaud PAM4 IMDD optical BTB system, respectively. In simulation C-band 25 GBaud PAM4 IMDD optical 20 km SSMF system, DPD can obtain 1 dB receiver sensitivity improvement for VFE at a BER for 1×10^{-3}; in C-band 20 GBaud PAM4 IMDD optical BTB system, DPD can obtain 2.4 dB and 1.2 dB receiver sensitivity improvement for FFE and VFE, respectively. Therefore, our DPD scheme can effectively improve the power budget of the PAM4 IMDD optical system.

REFERENCES

[1] K. Zhong, X. Zhou, J. Huo, et al. "Digital signal processing for short-reach optical communications: A review of current technologies and future trends." Journal of Lightwave Technology 36.2 (2018): 377-400.

[2] X. Tang, et al. "C-band 56-Gb/s PAM4 transmission over 80-km SSMF with electrical equalization at receiver." Optics express 27.18 (2019): 25708-25717.

[3] M. Zhu, et al. "Experimental Demonstration of 80-Gb/s DSB OOK Signal Transmission Over 100-km SSMF with Simplified Volterra Based DFE." 2021 Opto-Electronics and Communications Conference (OECC). IEEE, 2021.

[4] X. Li, S. Faruk, and S. J. Savory. "Advanced nonlinear digital signal processing for short-reach applications." Optical Fiber Communication Conference. Optica Publishing Group, 2021.

[5] S. Liu, et al. "Non-Orthogonal DMT Enabled by Iterative ICI Cancellation Algorithm for Bandwidth-Limited IM/DD Optical Systems." Journal of Lightwave Technology 40.9 (2022): 2799-2806.

[6] J. Zhang, et al. "Demonstration of 100-Gb/s/λ PAM-4 transmission over 45-km SSMF using one 10G-class DML in the C-band." Optical Fiber Communication Conference. Optical Society of America, 2019.

[7] IEEE Standard for Ethernet Amendment 9: Physical Layer Specifications and Management Parameters for 25 Gb/s and 50 Gb/s Passive Optical Networks, IEEE Std 802.3ca-2020, pp. 1–267, Jul. 2020.

[8] R. Bonk et al., "50G-PON: The First ITU-T Higher-Speed PON System," IEEE Commun. Mag., vol. 60, no. 3, pp. 48–54, Mar. 2022.

[9] L. Huang, et al. "Performance and complexity analysis of conventional and deep learning equalizers for the high-speed IMDD PON." Journal of Lightwave Technology 40.14 (2022): 4528-4538.

[10] A. Napoli, et al. "Digital predistortion techniques for finite extinction ratio IQ Mach–Zehnder modulators." Journal of Lightwave Technology 35.19 (2017): 4289-4296.

[11] G. Li, et al. "Performance Assessments of Joint Linear and Nonlinear Pre-Equalization Schemes in Next Generation IMDD PON." Journal of Lightwave Technology 40.16 (2022): 5478-5489.

[12] H. Jiang, et al. "Digital Pre-Distortion Using Gauss-Newton Based Direct Learning Architecture for Coherent Optical Transmitters." (2023).